Available online at www.sciencedirect.com
SCIENCE DIRECT
Journal of Electrostatics 64 (2006) 699–705
Journal of ELECTROSTATICS
www.elsevier.com/locate/elstat

A wire-to-wire type nonthermal plasma reactor with ferroelectric pellet barrier

Jae-Duk Moon

School of Electronic and Electrical Engineering, Kyungpook National University, 1370 Sankyuk-Dong, Buk-Gu, Daegu 702-701, South Korea

Received 23 March 2004; received in revised form 23 July 2004; accepted 7 January 2006
Available online 9 February 2006

Abstract

A new wire-to-wire type of discharge plasma reactor with ferroelectric pellet barrier has been proposed and investigated experimentally. It was found that there were intense microdischarge currents taking place on the AC corona-charged surfaces of the ferroelectric pellet barrier. These surfaces were placed on the bottom wire electrode in the reactor. This type of nonthermal plasma reactor was found to generate a corona discharge twice per half cycle of the applied AC high voltage, once from the upper corona wire and again from the surface of the pellet barrier.

As a result, the proposed plasma reactor has the potential to greatly increase ozone production and may find use as an effective means for removing pollutant gases.
© 2006 Elsevier B.V. All rights reserved.

Keywords: Nonthermal plasma reactor; Wire-to-wire; Ferroelectric pellet barrier; Electrophysicochemical reaction; Ozone generation

1. Introduction

Acid rain, global warming, ozone depletion, and smog are preeminent environmental problems facing the world today. Nonthermal discharge plasma techniques offer an innovative approach to the cost-effective solution of these problems [1–6]. Several nonthermal discharge plasma techniques have been proposed for the removal of NO_x, SO_x, volatile organic carbons (VOCs), and chlorofluorocarbons (CFCs) from pollutant gases [7]. These include the production of nonthermal discharge plasma using a pulsed corona discharge [1,7–9], silent or dielectric barrier discharge [7,10,11], surface discharge [12,13], and corona discharge in a ferroelectric pellet barrier [7,14,15]. The effective removal of NO_x, SO_x, and VOCs from pollutant gases, however, requires the generation of an intense corona discharge in the processing region of the plasma reactor [5,7]. Consequently, most of the electrical energy fed to the reactor has to supply the production of energetic electrons instead of heating the ambient gases and ions in the processing space [7]. The removal of pollutant gases can be stimulated by an electrophysicochemical reaction [5,7]. This electrophysical reaction originates from the energetic electrons [5,7,14,15], where the electrochemical reaction is mainly caused by the ozone and radicals produced from corona discharge in a nonthermal discharge plasma reactor [7–9]. Effective ozone generation is the key technology in making nonthermal plasma reactors practical and effective for removing pollutant gases [7–9].

The ferroelectric pellet, packed-bed discharge plasma reactor is sometimes used to remove pollutant gases. This type of reactor has proven to be effective because it produces a dense discharge plasma [16–18]. When an AC voltage is applied to ferroelectric pellet, packed-bed reactor, the pellets become polarized, and a strong electric field is formed at the top and bottom contact points of the ferroelectric pellets. Thus, the surfaces of each pellet become the sites of intense corona discharge. Due to the very compact spacing in the packed pellet bed, the thermal energy from the intense corona discharges greatly elevates the temperature in the reaction space. The lifetime of the ozone thus becomes very short, and only a small amount of ozone remains to react with pollutant gases [19,20]. As a result, the overall efficiency of removing pollutant gases

E-mail address: jdmoon@knu.ac.kr.

0304-3886/$ - see front matter © 2006 Elsevier B.V. All rights reserved.
doi:10.1016/j.elstat.2006.01.005

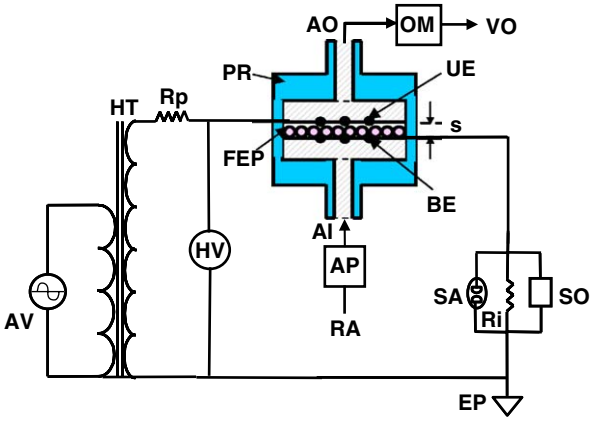
decreases greatly, such that the efficiency becomes insufficient for application to large-scale industries [7].

In this paper, we describe a wire-to-wire type of discharge plasma reactor with ferroelectric pellet barrier. This proposed configuration has been investigated experimentally. Intensive microdischarge occurs on the AC corona-charged surfaces of the ferroelectric pellet barrier placed on the bottom wire electrode of the wire-to-wire system. We report on the current–voltage and ozone generation characteristics of the reactor, both with and without the ferroelectric pellet barrier. The oscilloscope plots of current versus time were analyzed for each case and their microdischarges are compared.

2. Experimental setup

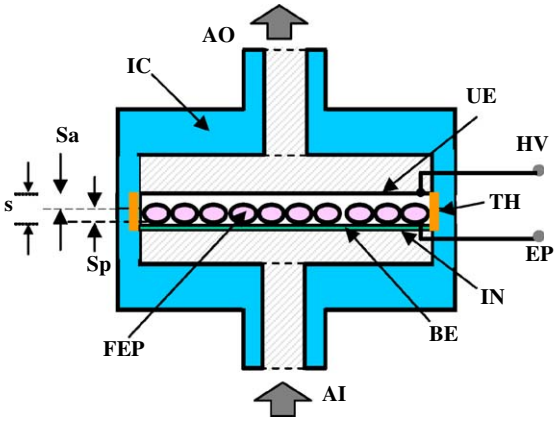
A schematic diagram of the experimental setup is shown in Fig. 1. The setup consists of the cylindrical nonthermal plasma reactor chamber (PR), a high-voltage AC power supply (AV, HT), air feeder (AP), ozone monitor (OM), and current and voltage measurement sets (HV, SO). The configuration of the reactor is a typical wire-to-wire type electrode system consisting of an upper electrode (UE), and a bottom electrode (BE). A ferroelectric pellet barrier (FEP) is installed on the bottom wire electrode.

Fig. 2 shows the closeup view of the reactor with the pellet barrier on the bottom side of the wire electrode. The ferroelectric pellet are 1.5-mm diameter titanium dioxide



AI	air inlet	PR	plasma reactor
AO	air outlet	RA	room air
AP	air pump	Ri	current resistor
AV	AC line voltage	Rp	protection resistor
BE	bottom wire electrode	s	airgap spacing
EP	earthed point	SA	surge arrester
FEP	ferroelectric pellet	SO	storage oscilloscope
HT	high volt transformer	UE	upper wire electrode
OM	ozone monitor	VO	air vent out
HV	digital voltmeter with high volt probe		

Fig. 1. Schematic diagram of the experimental setup.



AI :	air inlet	IN :	insulator net
AO :	air outlet	s :	total gap spacing
BE :	bottom wire electrode	Sa :	air gap spacing
EP :	earthed terminal	Sp :	Diameter of pellet
FEP :	ferroelectric pellet	TH :	teflon supporting holder
HV :	ac high volt terminal	UE :	upper wire electrode
IC :	insulation cylindrical case		

Fig. 2. Configuration of proposed plasma reactor with pellet barrier.

(TiO_2, $\varepsilon_r = 150$, $\rho = 50\,G\Omega\,m$). The pellets are set on an insulator net (IN) to prevent them from falling into the space below the bottom corona wire. The airgap spacing s is defined as the sum of the air gap S_a and the pellet diameter S_p, i.e. $s = S_a + S_p$. The air gap S_a between the upper corona wire electrode and the tops of the titanium pellets is set so that a spatial corona discharge occurs in the air gap. Room air (RA) is fed as the input gas via the input port (AI) using an air pump (AP). The input gas is vented to the output port (AO).

Fig. 3 illustrates the upper and bottom wire electrodes, both of 0.2-mm diameter 30-cm long stainless-steel. Three types of electrode were used in the experiments. These variations consisted of (a) 1-line wire electrode, (b) 3-line wire electrode, and (c) 5-line wire electrode. All electrodes were placed in the 30 mm × 30 mm reaction zone using a 50 mm wide, 1-mm thick Teflon sheet. The two-wire electrode holders were set with an air gap spacing s.

An adjustable, 0 to 20-kV, 60-Hz AC voltage was applied between the wire electrodes. The voltage was monitored using a Fluke 75 digital voltmeter and Tektronix P6015A, 1000:1 high-voltage probe, as shown in Fig. 1. Corona current was measured using a 10-kΩ, metal-film shunt resistor R_i with surge arrestor (SA) and Fluke 75 digital voltmeters. The high-voltage and corona-current waveforms were observed using a Tektronix TDS 340A storage oscilloscope (SO), again as shown in Fig. 1. The ozone concentration from the AO of the reactor was measured using OM, Dasibi DY 1500. Room air at 20 °C and 50% RH was fed to the IP of the reactor by an AP at a constant flow rate of 2 l/min.

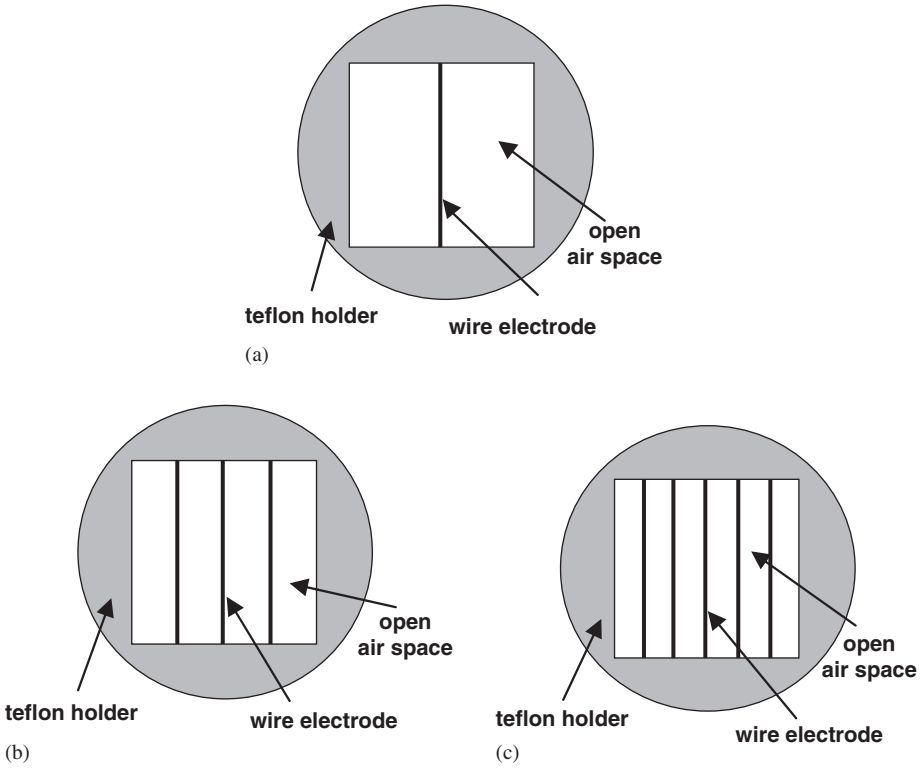


Fig. 3. Configuration of the corona electrodes tested.

With this type of electrode configuration, a processing space of dimension S_a exists in between the corona wire and the pellet barrier. The generated ozone can spread out over this region, where the temperature is relatively low compared with the space within the ferroelectric packed pellet bed. The pollutant gases can be treated more effectively in this processing space than is possible without the packed bed.

3. Results and discussion

Fig. 4 shows the measured current–voltage (I–V) characteristics of the plasma reactor, both with and without the pellet barrier. Below about 6.5 kV, both currents increased slowly and linearly with increasing input voltage. These displacement currents are caused by the reactor's capacitive load. The corona characteristics without the pellet barrier exhibited a rapid increase and eventual breakdown as the input voltage increased to above 7.5 kV. This result was observed for all three types of corona electrode described above. *I–V* characteristics with the pellet barrier differed significantly from those observed without a pellet barrier. Specifically, the corona current increased more slowly with increasing input voltage, reaching peak corona currents of up to 37, 46, and 82 μA at voltages of about 10.6, 9.7, and 9.2 kV, respectively for the one-, three-, and five-line wire-electrode configurations.

The corona onset voltages without the pellet barrier were all about 7.2 to 7.6 kV for each of the three types of wire electrodes, with a slight increase in onset voltage with increasing number of wires. With the pellet barrier, the corona onset voltages of the three-electrode configurations were somewhat reduced to the range of about 6.5 to 7.5 kV. In this latter case, the onset voltages *decreased* slightly with increasing number of corona wires.

This latter result might be explained in the following way: When a corona discharge originates on the upper wire electrode, the ions migrate toward are attached to the top surfaces of the pellets. The charge relaxation time constant, given by $\rho\varepsilon_0\varepsilon_r = 66$ s for TiO_2, is very long compared to the period of the 60-Hz AC source voltage. The charges deposited on top of the pellet thus cannot be dissipated within the short time available of a single cycle of the AC voltage. Hence they remain on top of the pellet and repel incoming ions of the same polarity. As a result, the corona onset voltage increases, as shown in Fig. 4(b). The same situation will also at the opposite polarity of the applied AC voltage.

Fig. 5 shows the oscilloscope traces of the AC high voltage and the corona currents of the 3-wire plasma reactor with and without the pellet barrier. As shown in Fig. 5(a), the corona discharge without the pellet barrier is weak for both positive and negative polarities ($I_p \approx 1.6$ mA averaged over 3 cycles), at a peak input voltage of about 7.4 kV. Conversely, with the pellet barrier included, corona discharge at both polarities is more intense ($I_p \approx 4$ mA averaged over 3 cycles) at the same 7.4-kV input voltage, as shown in Fig. 5(b).

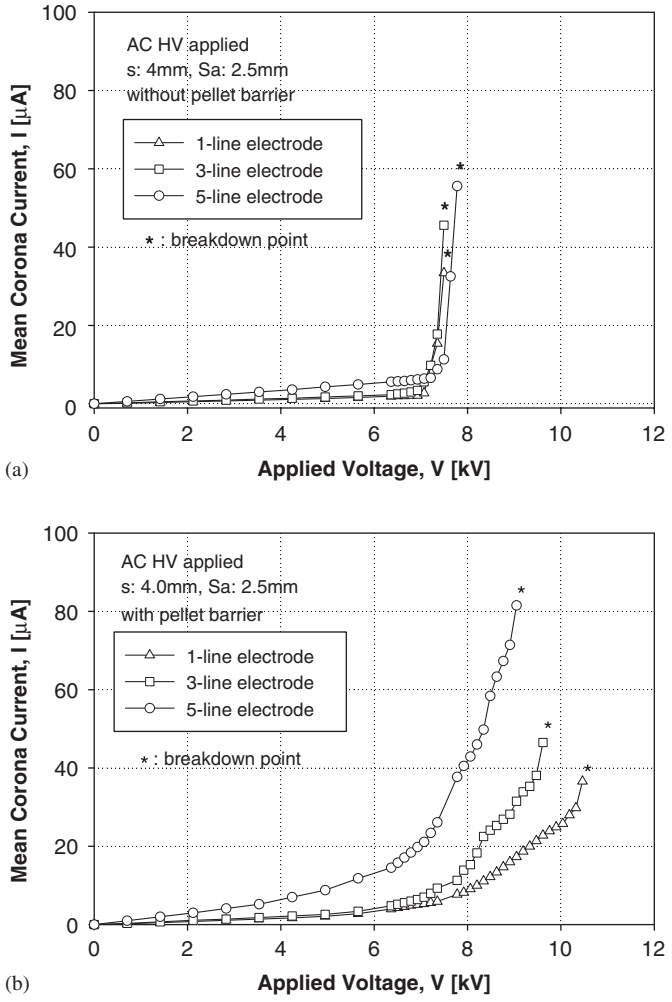


Fig. 4. *I–V* characteristics of proposed plasma reactor with and without pellet barrier.

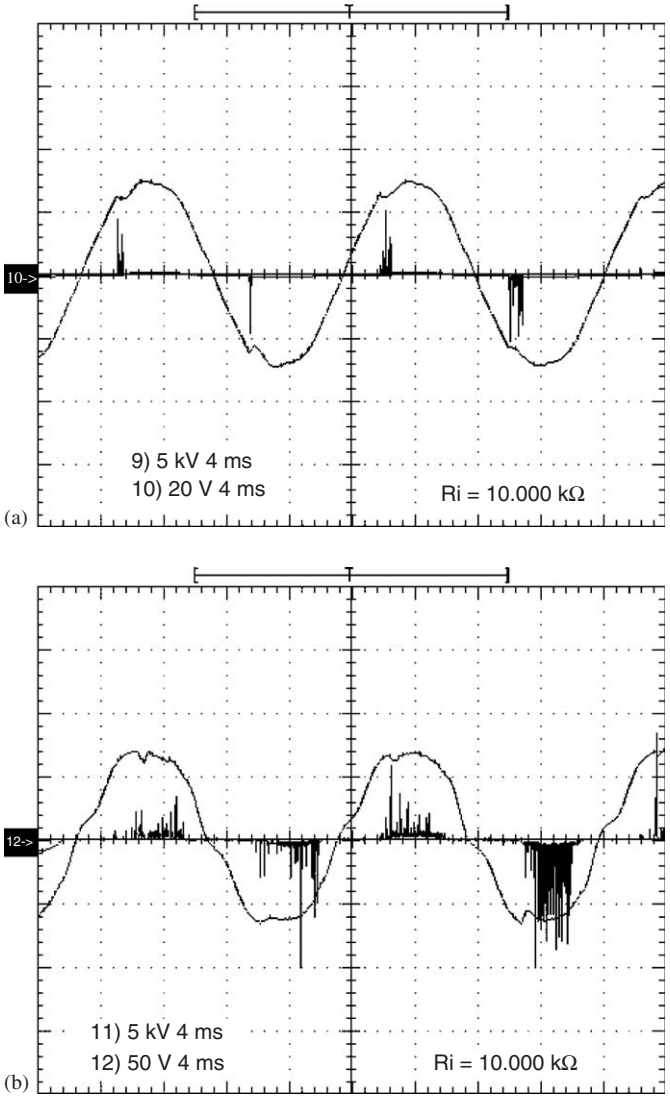
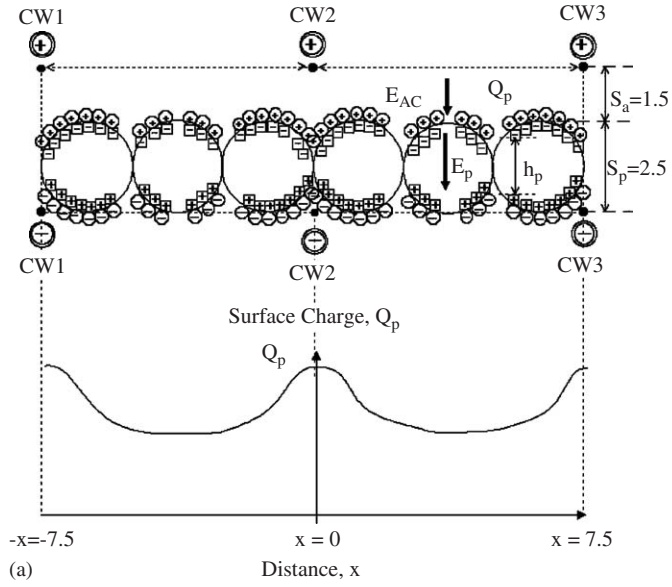


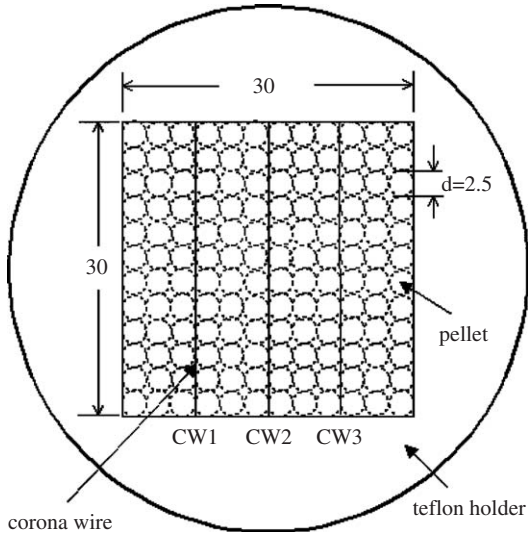
Fig. 5. Oscilloscope traces of corona current and AC voltage of proposed plasma reactor with and without pellet barrier.

Fig. 6 shows the proposed charge distribution with the pellet array under the upper side of the 3-line corona wire electrode. If charge Q_t is stored on the top of a pellet, an opposite charge $-Q_t$ will be induced on the bottom surface of the pellet. A charge-induced voltage $V = Q_t/C$ will then appear across the top and bottom surfaces of the pellets, where C is the capacitance of the pellet. If the amount of charge is increased, the fields at the top and bottom of every pellet will become strong.

In this experiment, the total ionic charge migrating from the corona wire to the bed surface is $Q_t = I_p t_p$. The average values of I_p and t_p over one half AC cycle without pellets can be obtained from Fig. 5(a), where $V_i = 16\,\text{V}$, $R_i = 10.00\,\text{k}\Omega$, $I_p = V_i/R_i \approx 1.6\,\text{mA}$, and $t_p \approx 0.8\,\text{ms}$. Thus $Q_t = I_p t_p = V_i t_p/R_i = 1.6\,\text{mA} \times 0.8\,\text{ms} = 1.28\,\mu\text{C}$. Due to the long relaxation time of the pellet and the repelling action of the accumulated charge on the pellet, the total charge Q_t is assumed to be spread uniformly over the tops of all 144 pellets in the discharge area, as shown in Figs. 6(a) and (b). The top surface charge Q_p on each individual can be estimated as $Q_p = Q_t/144$, which results in $Q_p = 8.9\,\text{nC}$. The voltage V_p across the diameter of each individual pellet can be estimated by $V_i = Q_p/C_p = 5.11\,\text{kV}$, where C_p is the pellet capacitance, given approximately by $C_p = \varepsilon_0\varepsilon_r A_p/h_p = 1.74\,\text{pF}$. The effective pellet area A_p is assumed to be given by $A_p = (d/6)^2\pi$, where $d = S_a = 2.5\,\text{mm}$ is the diameter of the pellet. Here h_p is the effective surface distance between the top and bottom charges across an individual pellet, assumed to be $h_p = d/6 = 0.42\,\text{mm}$ in this present case, as shown in Fig. 6(a). Using these various estimates, the field intensity E_p at the pellet surface can be calculated approximately from $E_p = V_p/h_p = 121\,\text{kV/cm}$. This value is very high compared to the air breakdown strength $E_a = 30\,\text{kV/cm}$ [21]. As a result, the charge on the top surface of the pellet can be discharged through the air to the bottom surface. In addition, many small partial discharges can be generated on the pellet [19], which could be the microdischarges [22] shown in Fig. 5(b).



(a)



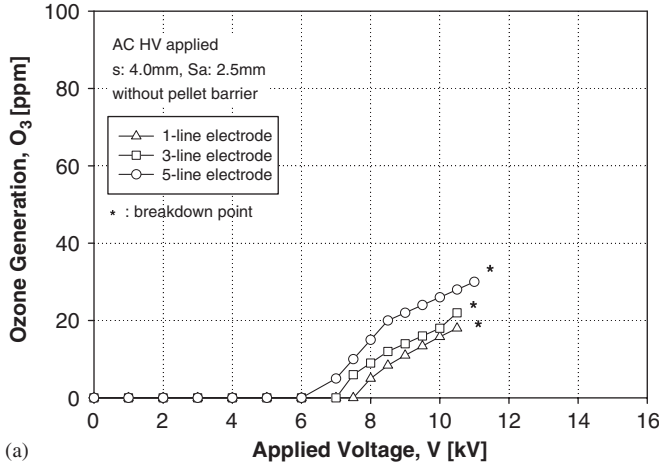
(b)

Fig. 6. Surface charge distribution and pellet position array of pellet barrier.

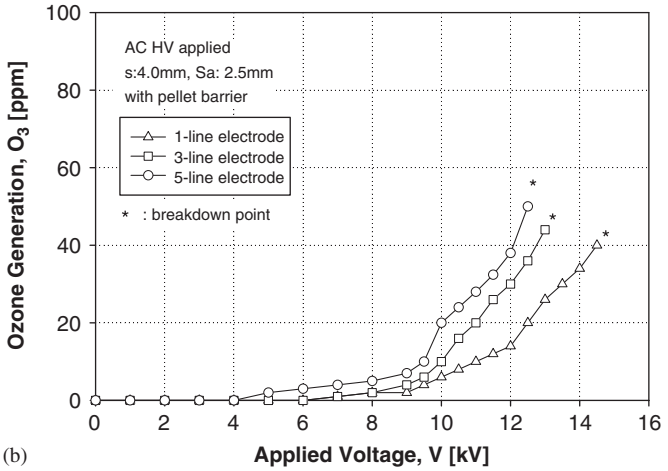
In addition, the effective electric field E_E on the top of the pellet will be further increased by the superposition of the AC power field E_{AC}, hence the effective field will really be given by $E_E = E_p + E_{AC} \gg E_a$, as shown in Fig. 6(a). The effective surface distance $h_p = d/6 = 0.42\,\text{mm}$ is a relatively small distance compared to the air gap spacing $S_a = 1.5\,\text{mm}$. This also indicates that it is difficult to have a discharge from the top of the pellet upward toward the upper corona wire.

This microdischarge-producing mechanism at the pellet surface, as it occurs over the first positive-going cycle of the AC voltage, would be the same as the second negative-going voltage cycle. Thus the surface discharge will occur during both the positive and negative-going cycles of each AC voltage cycle. During the second half of the negative-going cycle, the previously deposited positive charge on the top of the pellet will have little tendency to discharge. As a result, the proposed microdischarge-occurring model [19,22] of the pellet surface discharge, which occurs from the top side charge to the bottom side charge of the pellet, should be valid for this estimation of the experimental conditions.

Fig. 7 shows the output ozone generation characteristics as a function of applied AC high voltage for both cases: with and without a pellet barrier, and also for the three types of wire electrodes. As the plots shown, ozone generation is initiated at the corona onset voltage, and increases with increasing voltage until a maximum value is reached near the breakdown voltage. Higher ozone concentration, with a maximum value of 53 ppm, was produced from the plasma reactor that included a ferroelectric pellet barrier. Without the barrier, the maximum measured ozone concentration was only 30 ppm. Ozone generation with the pellet bed is thus increased by a factor of about 1.8. This result is attributable to the intense microdischarges that occur at the top surfaces of the ferroelectric pellets [22].



(a)



(b)

Fig. 7. Ozone generation characteristics of proposed plasma reactor with and without pellet barrier.

Our observed results suggest that a wire-to-wire type plasma reactor with ferroelectric pellet barrier generates corona discharge twice for every half-cycle of the applied AC voltage, once from the corona wire electrode (known as a "spatial" corona discharge) [4,7] and a second time from the surface of the pellets of the barrier (known as "pellet-bed" corona discharge) [7,16–18]. The wire-to-wire type discharge plasma reactor, including a ferroelectric pellet barrier, may find use as an effective plasma reactor for the removal of pollutant gases.

4. Conclusion

The great concern over air pollution has stimulated the development of new and more effective gas-cleaning techniques. Several methods have been proposed as effective techniques for removing pollutant gases.

In this paper, a new wire-to-wire type of discharge plasma reactor with a ferroelectric pellet barrier has been proposed and investigated experimentally with a focus on the feasibility of using it as an effective plasma reactor. The following observations have been made:

1. Intense microdischarge currents occurred over the AC-corona-charged top surface of the ferroelectric pellet barrier. The latter was placed on the bottom corona wire electrode.
2. The wire-to-wire type of discharge plasma reactor with ferroelectric pellet barrier generated corona discharge twice per each half-cycle of applied AC voltage, once from the corona wire electrode (known as a spatial corona discharge), and a second time from the surface of the pellets of the barrier (known as pellet-bed corona discharge).
3. The experimental plasma reactor produced 1.8 times the ozone as that obtained without the pellet barrier.

5. Summary

A new wire-to-wire type of discharge plasma reactor with a ferroelectric pellet barrier has been proposed and investigated experimentally with a focus on the feasibility of using it as an effective plasma reactor. There were intense microdischarge currents that took place on the AC corona-charged top surface of the ferroelectric pellet barrier which was placed on the bottom corona wire electrode in the proposed plasma reactor. This wire-to-wire type of discharge plasma reactor with a ferroelectric pellet barrier could generate corona discharge twice per every half cycle of AC voltage applied, once from the corona wire electrode and a second time from the surface of the pellets of the barrier.

As a result, the proposed plasma reactor could produce a greatly increased ozone, 1.8 times that without the pellet barrier. This wire-to-wire type of discharge plasma reactor, with ferroelectric pellet barrier, could be used as a means for the effective removal of pollutant gases.

Acknowledgement

This work was financially supported by MOCIE through EIRC program, Korea.

References

[1] K. Yan, Corona Plasma Generation, Eindhoven, 2001.
[2] M.L. Balmer, G. Fisher, J. Hoard, Nonthermal plasma for exhaust emission control: NO_x, HC, and particulates, ISBN 0-7680-0490-X, USA (1999).
[3] J.-S. Chang, A.J. Kelly, J.M. Crowley, Handbook of Electrostatic Processes, Marcell Dekker, New York, 1995.
[4] H.H. Kim, G. Prieto, K. Takashima, S. Katsura, A. Mizuno, Performance evaluation of discharge plasma process for gaseous pollutant removal, J. Electrostatics 55 (2002) 25–41.
[5] B.M. Penetrante, and S.E. Schultheis, Nonthermal plasma techniques for pollution control, Spring, Berlin, Heidelberg, NATO ASI Series 34, A&G, 1993.
[6] U. Kogelschatz, Ozone generation and dust collection, in: E.M. van Veldhuizen (Ed.), Electrical Discharge for Environmental Purposes: Fundamentals and Applications, Nova Science Publishers, New York, 2000.
[7] NATO Advanced Research Workshop on Nonthermal Plasma Techniques for Pollution Control, Cambridge University, England, UK, 21–25 September 1992, pp. 1-8.
[8] R.H. Amirov, E.I. Asinovsky, I.S. Samoilov, A.V. Shepelin, Oxidation characteristics of nitrogen monoxide by nanosecond pulse corona discharges in a methane combustion flue gas, Plasma Sources Sci. Technol. 2 (1993) 289–295.
[9] G. Sathiamoorthy, S. Kalyana, W.C. Finney, R.J. Clark, B.R. Locke, Chemical reaction kinetics and reactor modeling of NO_x removal in a pulsed streamer corona discharge reactor, Ind. Eng. Chem. Res. 38 (5) (1999) 1844–1855.
[10] L.A. Rosocha, G.K. Anderson, L.A. Bechtold, J.J. Coogan, H.G. Heck, M. Kang, W.H. McCulla, R.A. Tennant, P.j. Wantuck, Treatment of hazardous organic wastes using silent discharge plasmas, NATO ASI series, Part B, 1993 pp. 281–308.
[11] W. Niessen, O. Wolf, R. Schuft, M. Naiger, The influence of ethane on the conversion of NO_x in a dielectric barrier discharge, J. Phys. D: Appl. Phys. 31 (1998) 542–550.
[12] S. Masuda, S. Hosogawa, X.-L. Tu, K. Sakakibara, S. Kitoh, S. Sakai, Destruction of gaseous pollutant by surface induced plasma chemical process (SPCS), IEEE Trans. Ind. Appl. 29 (4) (1993) 781–786.
[13] T. Oda, R. Yamashita, I. Haga, T. Takahashi, S. Masuda, Decomposition of gaseous organic contaminants by surface discharge induced plasma chemical processing-SPCP, IEEE Trans. Ind. Appl. 32 (1) (1996) 118–123.
[14] H. Mätzing, H.R. Paur, Chemical mechanism and process parameters of flue gas cleaning by electron beam, in: J.O. Nriagu (Ed.), Gaseous Pollutants: Characterization and Cycling, Wiley Series in Advances in Environmental Science and Technology, vol. 24, 1992 pp. 307–333.
[15] M.G. Nickelsen, W.J. Cooper, C. Kurucz, T. Waite, Removal of benzene and selected alkyl substituted benzene from aqueous solution utilizing continuous electron radiation, Environ. Sci. Technol. 26 (1992) 144–152.
[16] T. Yamamoto, Decomposition of Toluene, o-Xylene, Trichloroethylene, and their mixture using a $BaTiO_3$ packed-bed plasma reactor, J. Adv. Technol. 1 (1) (1996) 67–78.

[17] K. Jogan, A. Mizuno, T. Yamamoto, J.-S. Chang, The effect of air mixture on the reduction of CO_2 from combustion flue gases by an AC ferroelectric packed bed plasma reactor, Pol. J. Appl. Chem. XXXIX (z4) (1995) 573–583.
[18] J.-D. Moon, S.-T. Geum, Discharge and ozone generation of a ferroelectric-ball/mica-sheet barrier, IEEE Trans. IA 34 (6) (1998) 1206–1211.
[19] J.-D. Moon, S.-T. Geum, G.-T. Lee, Corona discharge and ozone generation characteristics of a point-plate type nonthermal plasma reactor with ferroelectric pellet barrier, J. Korean Phys. Soc. 38 (6) (2001) 680–685.
[20] J.-D. Moon, G.-T. Lee, S.-T. Geum, Discharge and NO_x removal characteristics of nonthermal plasma reactor with a heated corona wire, J. Electrostatics 50 (2000) 1–15.
[21] J.D. Cobine, Gaseous Conductors, Dover, New York, 1958, pp. 173–177.
[22] D. Braun, U. Küchler, G. Pietsch, Microdischarge in air-fed ozonizers, J. Phys. D: Appl. Phys. 24 (1991) 564–572.